A Unidirectional Traveling-Wave Optical Maser*

By J. E. GEUSIC and H. E. D. SCOVIL

(Manuscript received March 20, 1962)

The basic ideas leading to a unidirectional traveling-wave optical maser are presented. Experimental data on the performance of pulsed ruby amplifying sections and high density PbO glass Faraday rotation isolators are given. Feasibility tests on a two-section device have been made and are in agreement with predictions. Some remarks are made concerning image definition, channel capacity, noise and pump power requirements.

I. INTRODUCTION

Net gain at optical frequencies was demonstrated by the successful operation of maser oscillators.[1,2] The first direct measurements of gain at optical frequencies were made by Javan, Bennett and Balik[3] for the helium-neon gas maser and by Kisliuk and Boyle[4] in a ruby solid state maser. The optical amplifiers described by these investigators were low-gain devices. Since at optical frequencies the maser is the only available amplifier which at present preserves amplitude and phase information, it may well have to provide extremely high stable gains of between 30–60 db in many applications, as for example in an optical communications system.

It is well known that to realize a stable high-gain amplifier it is essential to make the amplifier nonreciprocal. This has been accomplished in the case of the microwave traveling-wave maser[5] but has not previously been reported at optical frequencies. The objective of this paper is to discuss the basic principles which are necessary for realizing a nonreciprocal optical amplifier and to report the successful operation of a pulsed unidirectional traveling-wave optical maser (TWOM) using ruby.

Also the image amplifying ability of the TWOM is discussed and demonstrated.

* This work was supported in part by the U. S. Army Signal Corps under Contract DA-36-039-sc-87340.

II. BASIC PRINCIPLES

Consider a multimode transmission line containing active maser material as shown in Fig. 1. Over the length shown, assume that the single-pass power gain is G_0, that it is reciprocal, and that at each end the power reflection coefficient is r. If $G_0 r < 1$, the amplifier is stable. For a ruby optical maser with an air interface, $r \approx 0.07$; hence such a device will exhibit a stable gain if $G < 14$. If an $r \approx 0.07$ is accepted as typical (it may be made much smaller by the use of antireflection coatings), then it is evident that a simple optical maser with a gain of $\approx$6 db is a very stable amplifier with very little regeneration. On the other hand if a gain of 30 db is required, then r must be <0.001. This is extremely difficult to achieve, and it is evident that a stable gain of 60 db is essentially impossible from such a device.

The optical traveling-wave maser (TWOM) shown in Fig. 2 is a device capable of achieving extremely high stable gains. The device consists of a succession of amplifying sections, each of which has a gain of 6 db for the typical figures given above. These sections are separated by nonreciprocal elements or isolators so that power is easily transmitted in the direction of the arrows but strongly attenuated in the reverse direction. In fact the reverse loss in db of the isolator is chosen to exceed twice the single-pass gain in db of an amplifying section.

A simple way to realize isolation is to use the optical equivalent of a microwave Faraday rotation isolator. The main differences are the frequency, the material used, and the fact that our transmission line can support many modes. One may use numerous materials for the nonreciprocal rotator. Although transparent ferromagnetics, ferrimagnetics or anti-ferromagnetics may be considered, many other classes of materials could also be used; for instance it is not even necessary to use a material with a permanent magnetic dipole moment. Diamagnetics may be employed since they also exhibit Faraday rotation. In fact, nonreciprocal rotation was first observed by Faraday in a diamagnetic glass.

In the microwave Faraday rotation isolator the plane of polarization is determined by the rectangular waveguide. In the optical counterpart a polarizing medium can be used to fulfill the same function. In addition to having nonreciprocal rotation and defining the plane of polarization,

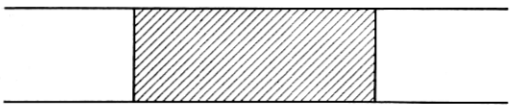

Fig. 1 — Transmission line containing an active maser material.

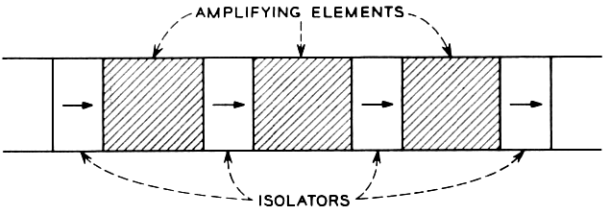

Fig. 2 — Schematic diagram of a unidirectional traveling-wave optical maser.

we need to be able to absorb waves with the unwanted polarization. In the microwave equivalent this is done by using a sheet of loss film placed so that its plane is parallel to the electric field of the wave which we wish to absorb. In the optical version this absorption may be combined in the polarizing medium itself if we use a material which has dichroic characteristics. The construction of an isolator is now straightforward and is shown in Fig. 3. In Fig. 3 a wave enters from the left-hand side with its plane of polarization defined by the dichroic polarizer as shown in the end view. The plane of polarization is rotated by 45° in the clockwise direction by the Faraday medium and passes through the right-hand polarizer. However, a wave entering the right-hand polarizer has its plane rotated 45° in the clockwise direction and hits the left-hand polarizer with its plane of polarization in the low transmittance or absorbing direction of the polarizer. The direction of the axially applied magnetic field with respect to the forward direction must be chosen in accordance with the sign of the Verdet constant of the Faraday medium used.

A TWOM may be built as shown in Fig. 4. In the figure the active medium is illuminated with pump power in one of several known ways. A two-section maser is shown; however, additional sections can be added.

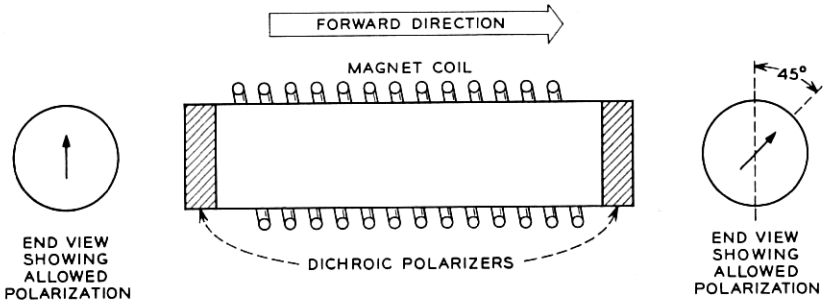

Fig. 3 — An optical Faraday rotation isolator.

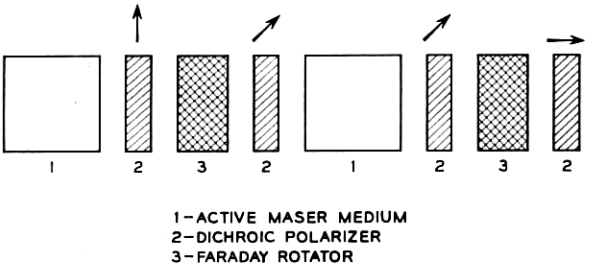

Fig. 4 — Elements in a two-stage TWOM.

For best operation, of course, all interfaces would have antireflection coatings. In the TWOM, alternate polarizers can be eliminated for simplicity.

An obvious application of the TWOM is as a power amplifier for an optical maser oscillator. Another application may be to obtain very high peak optical powers. It is well known that because of its energy storage the peak power of a maser may greatly exceed its average power. In fact some of the pulsed characteristics of a TWM have been analyzed.[6] The interaction of high optical power levels with matter will certainly allow many new and interesting phenomena to be studied. A focused beam with these peak intensities should have application to microwelding or micro-cutting of materials. Finally the TWOM may find application to amplify received signals in an optical relay system.

This concludes the discussion of the general ideas relating to a unidirectional traveling-wave optical maser. The concepts apply to either a CW amplifier or a pulsed amplifier. It now remains to discuss in more detail the theory and design of the individual amplifying sections and the optical isolators which have been used and tested in a pulsed ruby TWOM.

III. THE AMPLIFYING SECTION

Consider two levels 1 and 2 as shown in Fig. 5 with populations N_1 and N_2 and degeneracies g_1 and g_2 respectively. Also assume that the sample interacts at the transition $1 \rightleftarrows 2$ with a beam incident in a direction θ and φ having an energy density per unit frequency range per unit solid angle given by $\rho(\nu,\theta,\varphi,\mathbf{P})$. Here ν is the frequency of the radiation, $\mathbf{P}$ is a vector which defines an independent state of polarization of the radiation and θ and φ are the polar and azimuthal angles of a spherical coordinate system fixed in our sample. For this situation

Condon and Shortly[7] give the net rate of emission for transitions $1 \rightleftarrows 2$ as

$$\frac{d\rho}{dt}(\nu,\theta,\varphi,\mathbf{P}) = W(\theta,\varphi,\mathbf{P}) \left\{ \frac{\rho(\nu,\theta,\mathbf{P})v^3}{\nu^2} (g_1N_2 - g_2N_1) + h\nu g_1N_2 \right\} g(\nu) \quad (1)$$

where $W(\theta,\varphi,\mathbf{P})$ is the probability per unit time per unit solid angle of a spontaneous transition from $2 \rightarrow 1$ with emission in a direction θ,φ and polarization $\mathbf{P}$.

$g(\nu)$ is the normalized line shape for the transition.

N_1 and N_2 are the number of atoms per unit volume in levels 1 and 2, and

ν is the velocity of wave propagation in the medium.

Equation (1) gives both the stimulated emission and the spontaneous emission per unit solid angle in a direction θ and φ. Equation (1) takes into account the anisotropy of the transition probability.

In order to find the gain or loss through the medium in a direction θ,φ at the $1 \rightleftarrows 2$ transition, the portion of (1) due to stimulated emission is integrated in the following manner,

$$\int_{\rho_0}^{\rho} \frac{d\rho(\nu,\theta,\varphi,\mathbf{P})}{\rho(\nu,\theta,\varphi,\mathbf{P})} = \int_0^{l(\theta,\varphi)/v} \frac{W(\theta,\varphi,\mathbf{P})v^3}{\nu^2} (g_1N_2 - g_2N_1)g(\nu)\, dt$$

where $\rho_0(\nu,\theta,\varphi,\mathbf{P})$ is the incident energy density and $l(\theta,\varphi)$ is the length of the medium in the direction considered. Hence the gain in db is given by

$$G_{\text{db}}(\nu,\theta,\varphi,\mathbf{P}) = (10 \log e) \left[W(\theta,\varphi,\mathbf{P}) \frac{\lambda_0^2 l(\theta,\varphi)}{\epsilon} (g_1N_2 - g_2N_1)g(\nu) \right]$$

where λ_0 is the free-space wavelength and ϵ the dielectric constant at

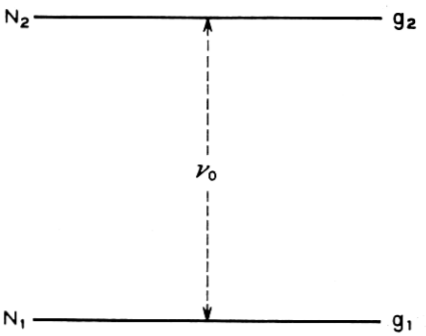

Fig. 5 — Two typical energy levels.

λ_0. For a Gaussian line shape, (approximately true for the ruby R_1 line at room temperature), the gain is given by

$$G_{\text{db}}(\nu,\theta,\varphi,\mathbf{P}) = (10 \log e)\left[W(\theta,\varphi,\mathbf{P})\frac{\lambda_0^2 l(\theta,\varphi)}{\epsilon}(g_1N_2 - g_2N_1)\right]\frac{2}{\Delta\nu} \cdot\sqrt{\frac{\ln 2}{\pi}}\exp -\frac{(\nu-\nu_0)^2}{(\Delta\nu)^2}4\ln 2 \tag{2}$$

where $\Delta\nu$ is the linewidth and ν_0 is the frequency at the center of the line. Using (2), the bandwidth B over which the gain is within 3 db of the peak gain is given by

$$B = B_M\sqrt{\frac{\log\dfrac{G_{\text{db max}}}{G_{\text{db max}}-3}}{\log 2}} \tag{3}$$

where $B_M = \Delta\nu$ (cf. equation (25) of Ref. 5). If the transition considered is isotropic (i.e. $W(\theta,\varphi,\mathbf{P}) = W$ = constant) then the gain given by (2) becomes

$$G_{\text{db}}(\nu,\theta,\varphi,\mathbf{P}) = (10 \log e)\left[\frac{\lambda_0^2 l(\theta,\varphi)}{8\pi\epsilon\tau}\right]\left(N_2 - \frac{g_2}{g_1}N_1\right)\frac{2}{\Delta\nu}\sqrt{\frac{\ln 2}{\pi}} \cdot\exp -\frac{(\nu-\nu_0)^2}{(\Delta\nu)^2}4\ln 2$$

where τ is the spontaneous emission lifetime for the transition and is equal to $(8\pi g_1 W)^{-1}$. From (2) or this last expression it is observed that the medium exhibits gain if $(g_1N_2 - g_2N_1) > 0$ and loss if $(g_1N_2 - g_2N_1) < 0$.

In the case of ruby at room temperature, inversion at the R_1 line (14,400 cm^{-1}) is obtained by maser operation as shown in Fig 6. Here we have lumped the blue and green bands as one level; this is of course an obvious oversimplification. Also the ground state is treated as a single level with degeneracy $g_1 = 4$. At room temperature this is a valid assumption since the linewidth of the R_1 and R_2 transition is large compared to the separation of the two zero field levels in the ground state. At lower temperatures the linewidths of the R_1 and R_2 transitions are small, so that the two zero-field levels of the ground state are resolved; then it is necessary to consider the ground state as two levels each with degeneracy 2. For ruby the time spent in the pumping states is negligible compared with the normal lifetime of the two metastable states shown, and the efficiency for atoms getting to the metastable states upon pumping into the green or blue bands is near 100 per cent. Based on this,

and assuming that pumping power is supplied for times short compared to the normal or stimulated emission lifetimes of the two metastable states, we can write

$$\frac{dN_1}{dt} \approx -fPN_1 \tag{4}$$

where P is the incident pumping power and f is a pumping efficiency factor, which depends on the pump transition probability and the properties of the electromagnetic structure used in the pumping process. Since we assume that the pump power P is supplied for a short time, (4) can be integrated to obtain

$$\begin{aligned} N_1 &= N \exp -f \int_0^t P dt \\ &= Ne^{-fE} \end{aligned} \tag{5}$$

where N is the total number of Cr^{3+} ions/cc in the ruby sample and E is the total energy absorbed by the material at the pumping transition. Now since it was assumed that the time spent in the pumping levels is negligible compared to the spontaneous lifetimes of the metastable

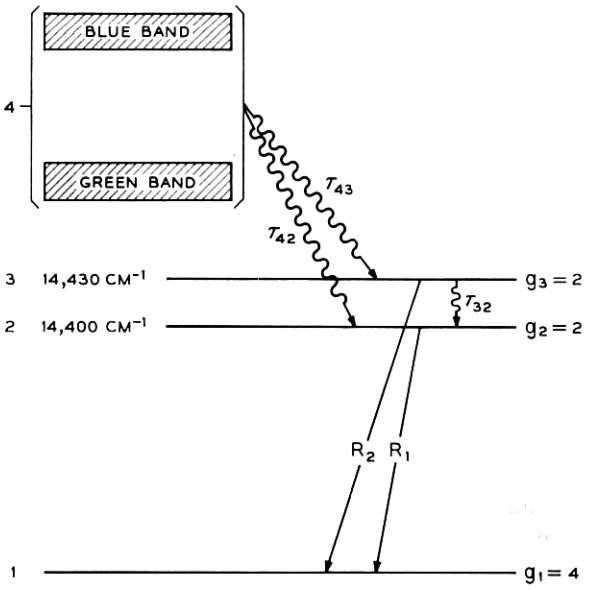

Fig. 6 — Optical energy levels of Cr^{3+} in Al_2O_3 .

states, the following relation holds,

$$N_1 + N_2 + N_3 \approx N \tag{6}$$

and $N_3 = \gamma N_2$ where γ is determined by τ_{42}, τ_{43} and τ_{23}. Using (2), the power gain G of the ruby material at the center of the ruby R_1 line when inverted is

$$G_{\text{db}} = A\left[N_2 - \frac{g_2}{g_1} N_1\right] \tag{7}$$

where

$$A = (10 \log e)\left[g_1 W(\theta,\varphi,\mathbf{P}) \frac{\lambda_0^2 l(\theta,\varphi)}{\epsilon}\right] \frac{2}{\Delta\nu} \sqrt{\frac{\ln 2}{\pi}}.$$

Upon substitution of (5) and (6) into (7) we obtain

$$\frac{G_{\text{db}}}{(L_{\text{db}})_{\max}} = \frac{1}{\frac{g_2}{g_1}(1+\gamma)}\left[1 - \left\{1 + \frac{g_2}{g_1}(1+\gamma)\right\} e^{-fE}\right] \tag{8}$$

where $(L_{\text{db}})_{\max}$ is equal numerically to the loss in db at the center of the line if all ions are in the ground state. To a good approximation this is equal to the loss through the unpumped material for a temperature T such that $kT \ll h\nu_{R_1}$, which is the case for the ruby R_1 line for temperatures 300°K and lower. Since (8) is derived for the case where the gain is measured in a time T_{meas} after the pump power has been supplied, which is short compared to τ_{21} and τ_{31} but long compared to τ_{43} and τ_{42}, the value of γ can be simply given for two limiting cases:

(a) $\tau_{23} < \tau_{42}$ and $\tau_{43} < T_{\text{meas}}$

$$\gamma = \exp h(\nu_{R_1} - \nu_{R_2})/KT.$$

At room temperature for ruby $\gamma = 0.865$

(b) τ_{42} and $\tau_{43} < T_{\text{meas}} < \tau_{23}$

$$\gamma = \frac{\tau_{42}}{\tau_{43}}.$$

At present no accurate data are available for ruby on the times τ_{23}, τ_{42} and τ_{43}; however, the measurements of Wieder[8] give upper limits for these times which indicate that case (a) is satisfied at room temperature. Also the gain measurements to be presented are consistent with the assumption $\gamma = 0.865$.

To determine what values of fE could be achieved and what gains

could be obtained for a pulsed ruby amplifying stage, gain measurements were carried out on an amplifying test section at room temperature. This test section consisted of a 3-inch long, 0.250-inch diameter, c-axis oriented (0.065 per cent by weight of Cr_2O_3 in Al_2O_3) ruby rod and a G.E. FT-91 Xenon flash tube located at the foci of a 3-inch long elliptical cylinder, as shown in Fig. 7. The gains were measured as is shown schematically in Fig. 8. The beam from a ruby oscillator was used as the signal source, and the gain or loss through the amplifying section was determined by measuring the ratio of the signal at the photomultiplier with and without the amplifier in the oscillator path. The measured loss through the unpumped amplifier at the peak of the R_1 line was 12 db. Because the ends of the ruby were not coated with antireflection layers, the measured gains had to be corrected to obtain the single-pass gain.

The expression for the numerical gain G of a reciprocal amplifier with feedback is given by

$$G = \frac{(1 - r)^2 G_0}{1 + r^2 G_0^2 - 2rG_0 \cos \varphi} \tag{9}$$

where r is the power reflection coefficient at each end and φ is the relative phase shift of a wave making one complete, round-trip traversal of the amplifier. Since the length of the ruby amplifier is not known to an

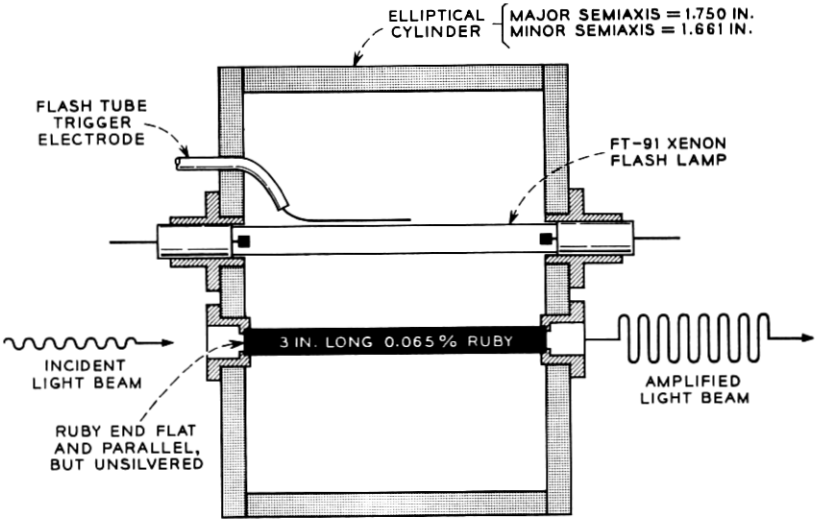

Fig. 7 — Ruby optical amplifier section.

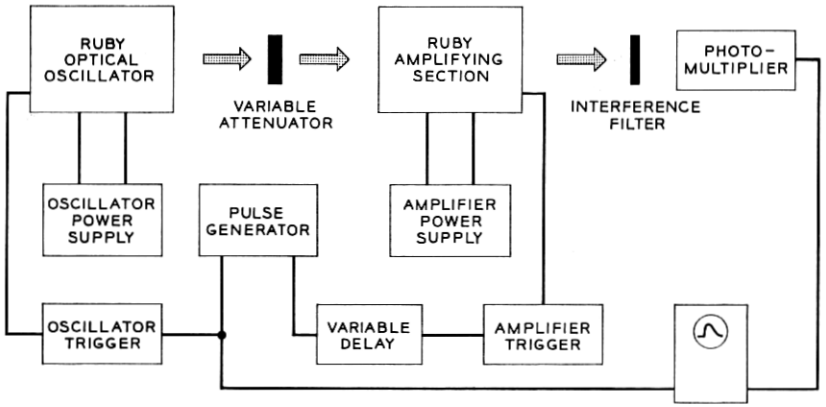

Fig. 8 — Schematic description of optical gain measurements.

accuracy better than a wavelength, the value of φ to be used in (9) to obtain the single-pass gain G_0 is not known. In the gain measurements an interference filter was used which had a passband larger than the ruby amplifying linewidth. Further, the measured bandwidth of a ruby oscillator is 1-2 kmc, whereas the separation of Fabry-Perot modes in our amplifying rod is

$$\Delta\nu \approx \frac{c}{2\sqrt{\epsilon}\, l} \approx 0.83 \text{ kmc.}$$

Hence it is reasonable to correct the data by assuming the proper gain formula to use in determining G_0 is one where G has been averaged over all possible values of φ. For the case where G is averaged we obtain

$$\bar{G} = \frac{(1 - r)^2 G_0}{(1 - G_0^2 r^2)}. \tag{10}$$

The experimental data corrected in this manner for the 3-inch long amplifying section are plotted in Fig. 9 along with the theoretical curve given by (8) for $\alpha = 0.865$, $g_1 = 4$ and $g_2 = 2$. Also plotted are data obtained on a 1-inch long ruby where the measured gains were smaller and the regeneration corrections needed to obtain the single-pass gain were less important. It is seen from Fig. 9 that our measured gain variation versus the input pumping parameter fE is in good agreement with the theory developed.

It remains to explain how the correlation between the values of fE on the abscissa of Fig. 9 and the measured light intensity at the green

and blue bands was obtained. For this purpose, the relative intensity at the green and blue bands versus electrical energy input to the flash lamp was measured photoelectrically. The absolute relation of this relative intensity to fE was then determined by observing at what value of light intensity unity gain (0 db) was achieved with the amplifier in place.

The maximum measured net gains for the amplifiers tested depended rather critically on the FT-91 tubes used; however, by selecting FT-91 flash tubes and operating them at input energies of 250 joules (which is approximately twice their rating) net gains of 10 db and 6 db were obtained respectively for two different amplifiers. All the measurements were made at room temperature. Higher gains per unit length could have easily been achieved by cooling, for it is known from the measurements of Schawlow and Devlin[9] that the linewidth of the ruby R_1 line

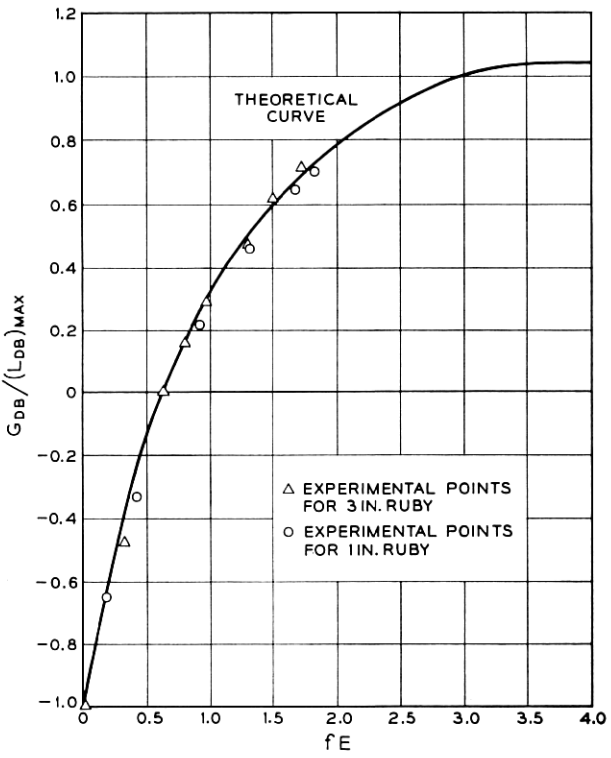

Fig. 9 — Gain versus input pump energy curve for a pulsed ruby maser at room temperature. $(L_{db})_{max}$ is 12 db and 4 db for the 3-inch and 1-inch ruby, respectively.

decreases quite rapidly with decreasing temperature between 300 and 80°K.

IV. THE OPTICAL ISOLATOR

To complete the discussion of the individual elements in the TWOM, it remains to discuss the basic principles involved in the design of an optical isolator and to report some performance data.

It is well known that the plane of polarization of a light beam, when passing through a Faraday medium, will be rotated by a magnetic field H applied to the material in a direction parallel to the direction of light propagation. The angular rotation θ of the plane of polarization is related to the strength of the magnetic field and the path length l in the medium by the expression

$$\theta = V \cdot H \cdot l \tag{11}$$

where the angle θ is chosen in the positive screw sense along the applied magnetic field. The constant of proportionality V is known as the Verdet constant and is a function of the material and the wavelength of light used. The Verdet constant is related to the material properties in the following manner

$$V = \pi\nu_0(N_+ - N_-)/Hc$$

where N_+ and N_- are the refractive indices for right- and left-handed circularly polarized light of frequency ν_0. In the case of ferromagnetics and antiferromagnetics, large Verdet constants have been measured. The large Verdet constant measured in each of these materials is due to the fact that the ions which produce the rotation see, in addition to the applied field, an internal field which is of the order of magnitude of the exchange field. Ferromagnetics would then be especially attractive. For the visible region of the optical spectrum, however, for ferromagnetics known to the authors, this large rotation is accompanied by large attenuation per unit length of material. This is because the absorption bands which give rise to the rotation in the ferromagnetic material usually extend from the ultraviolet well into the visible. However, ferromagnetic materials should be useful rotators in the infrared — i.e., beyond about 1μ.

The problem of building a good isolator in the visible (particularly at the R_1 line) depends upon finding a material which has a Verdet constant large enough to produce 45° rotation with reasonable fields and lengths, and which has low attenuation in the length of material which must

be used. For the ruby R_1 line at 14,400 cm^{-1}, known ferromagnetics are at present unsatisfactory. However, two diamagnetic materials appear to be good choices. One of these, ZnS(β), has a Verdet constant of 0.22 minute/cm/gauss at the R_1 line in ruby and is essentially transparent at this wavelength. For ZnS(β) a rotation of 45° requires a magnetic field of 3100 gauss for a 4-cm length. The second material, high-density PbO glass, also is attractive since it has a Verdet constant of 0.09 minute/cm/gauss at the R_1 line and an attenuation of 0.08 db/cm. Because of the commercial availability of the PbO glass from Corning Glass Works, this material was chosen for use in the optical isolator. In both the ZnS(β) and the PbO glass it is the Zn^{++} and Pb^{++} ions which are probably responsible for the rotation. In the PbO glass the absorption band which produces the rotation rises sharply at 4000 A, and extends to shorter wavelengths; this band is probably composed of the $^1S_0$ to $^3P_0$, $^3P_1$, $^3P_2$ transitions in the free-ion notation. Since the configuration which gives rise to $^3P_0$, $^3P_1$ and $^3P_2$ states in the free ion contains bonding electrons in the solid state, the transition observed beyond 4000 A should more properly be referred to as a charge transfer band. This tentative assignment seems supported by measurements made on Pb^{++} in CaO by Ewles as discussed by McClure.[10] The Verdet constant and the attenuation per unit length have been measured for Corning #8363 high PbO content glass as a function of wavelength and are shown in Fig. 10. The data in Fig. 10 indicate that PbO glass is a useful Faraday rotator for optical isolators in the wavelength range 5000–7000 A.

To define the plane of polarization in the isolator and to provide reverse loss, as was discussed earlier, dichroic polarizers such as Tourmaline and Polaroid sheet or crystal polarizers such as Nicol prisms and Glan-Thomson prisms can be used. At the R_1 line, type HN-38 Polaroid sheet is a good choice, having a transmittance of 0.86 for the parallel orientation and a transmittance of approximately 0.01 for the perpendicular orientation.

An optical isolator was constructed in the manner as depicted in Fig. 3. A 4-inch long, $\frac{1}{2}$-inch diameter PbO glass rod was used as the rotator, and Type HN-38 Polaroid polarizers were used to define the plane of polarization and to provide reverse loss. A water-cooled solenoid provided the necessary field to produce 45° rotation. The reverse loss of the isolator was measured at the R_1 (14,400 cm^{-1}) line and was found to be approximately 16 db. The measured insertion loss of the isolator was 3 db. In this isolator, optimized operation has not been realized; however, measurements on the individual components were made to determine the best performance that can be achieved with a more carefully con-

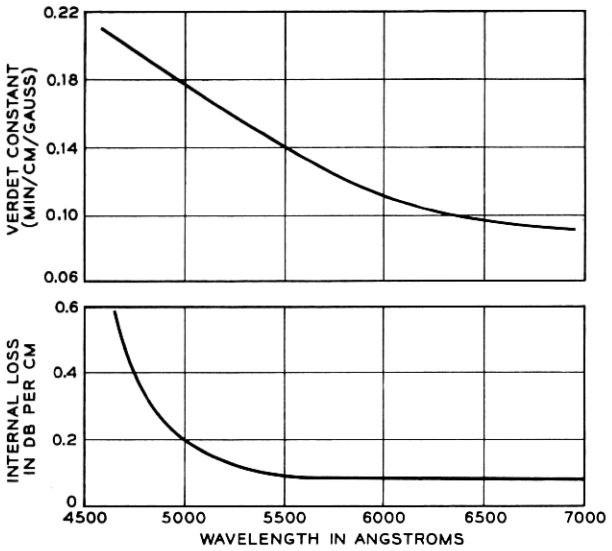

Fig. 10 — Variation of the Verdet constant and the internal loss of PbO glass versus wavelength.

structed isolator. These measurements on the individual components indicate that an isolator with an insertion loss of 1 db and a reverse loss of 15 to 17 db could be realized if antireflection coatings are used on all isolator surfaces.

V. OPTICAL TRAVELING-WAVE MASER PERFORMANCE

To test the feasibility of a high-gain (30–60 db) optical amplifier a test TWOM was assembled, consisting of two amplifiers separated by an isolator section. The two individual amplifiers had net gains of 10 db and 6 db respectively, and the isolator had an insertion loss of 3 db. A net gain of 13 db was expected. The measured net gain was 12.2 db; the discrepancy of 0.8 was probably due to the lack of perfect alignment. The oscillogram presentation of the gain of the amplifier is shown in Fig. 11. The top trace is the signal due to the oscillator alone as observed with the photomultiplier, with the TWOM out of the beam path. The middle trace shows the signal after amplification by the first amplifying stage with the isolator and second amplifier out of the beam path. Taking into account the changes made in the gain of the oscilloscope, the second trace indicates a net gain of 10 db through the first amplifier. The bottom trace shows the signal after passing through the

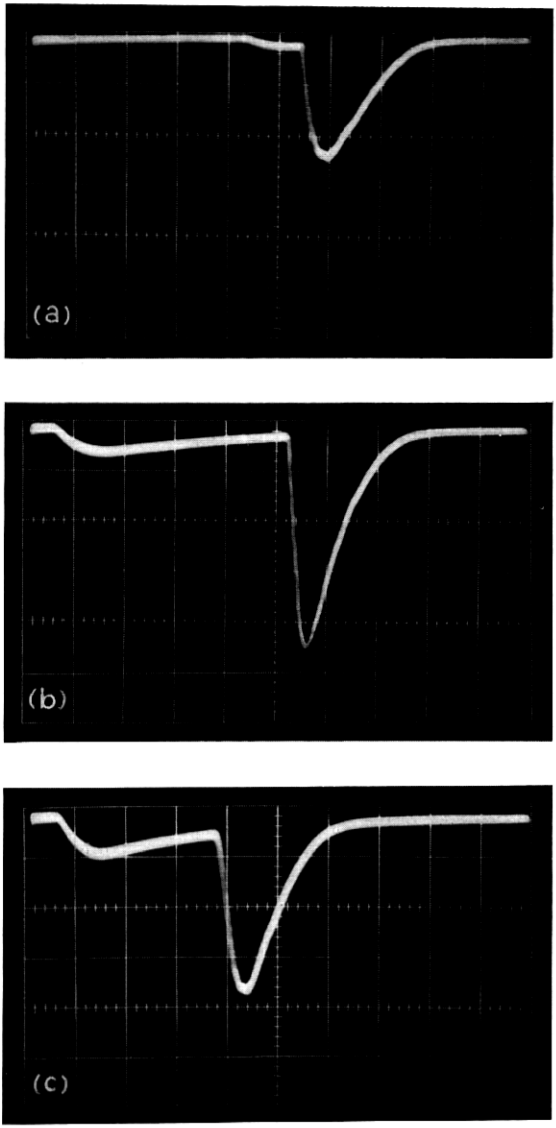

Fig. 11 — Oscilloscope photographs showing gain in the TWOM: (a) upper trace shows the signal at the photomultiplier due to the oscillator alone with the TWOM removed from the beam. Scope gain is 2 volts/cm. (b) Middle trace is the received photomultiplier signal with the first amplifier in the beam. Scope gain is 10 volts/cm. (c) The lower trace shows the oscillator signal as amplified by the entire TWOM. Scope gain is 10 volts/cm with 3 db of optical attenuation added. The sweep time is 100 microseconds/cm in all three traces.

entire TWOM. For this measurement 3 db of optical attenuation was introduced, and if this is taken into account the net gain of the TWOM was found to be 12.2 db.

In making all the gain measurements reported, a time constant was used so that individual oscillator spikes were not observed. A measurement of the gain with a shorter time constant did not contradict the measured peak gains observed (over the oscillator duration) with the longer time constant and also did not reveal any new spikes that were not present in the oscillator. In all the measurements the firing of the oscillator flash tube was delayed with respect to the firing of the amplifier pumping tubes; this was done so that the amplifier could build up to full gain before the probing signal was sent through the amplifier. In Fig. 11 this delay was approximately 400 microseconds. There was about a ± 50-microsecond jitter in firing the oscillator, and this accounts for the difference in position of the signal in the three traces shown in Fig. 11. The total physical length of the test TWOM was approximately 20 inches, with the isolator solenoid presently being the most space-consuming element. A shorter physical length is possible with a more careful and sophisticated design.

Inasmuch as the diameter of the ruby rods used in the amplifiers is 0.250 inch, the TWOM that has been described is a multimode amplifier capable of handling approximately 10^8 spatial modes. The fact that it can support 10^8 spatial modes suggests that image information can be sent through the amplifier. That is to say, the TWOM can be considered to be a limited aperture, infinite focal length lens with gain. To show that an image could be sent through a TWOM and amplified, a projection slide having on it a number of dark lines was placed before the input of the TWOM (in this case the second amplifier was removed for simplicity) and illuminated with the oscillator beam. The slide was then viewed with a lens and a camera as shown in Fig. 12. In Fig. 13 are shown

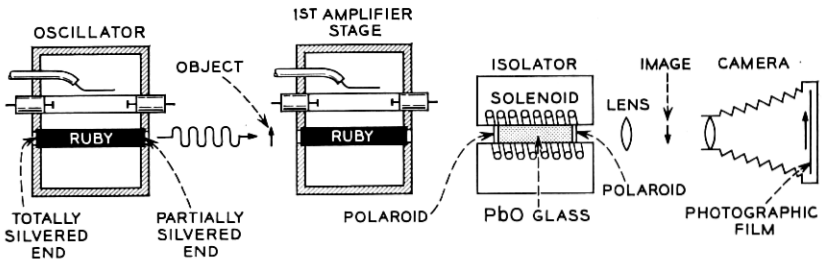

Fig. 12 — Schematic description of the image amplification experiment.

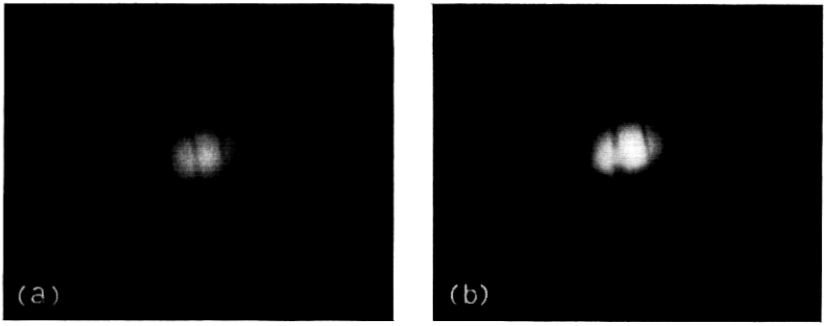

Fig. 13 — Photographs showing image amplification in the TWOM: (a) This photograph shows the observed image of two lines on the object slide as observed with unity gain. (b) This photograph shows the image when observed with the TWOM at a gain of approximately 5 db.

two pictures of this slide as taken through the TWOM. Only two bars on the slide were illuminated by the oscillator. The left photograph was made with the amplifier operated at unity gain, and the right photograph was made with an amplifier gain of approximately 5 db. It is seen that there is greater contrast in the amplified image than in the unamplified image. A quantitative measurement of the photographic negative with a densitometer showed a gain of approximately 4 db in the amplified image over the unamplified image. Although admittedly the observed image amplification is quite crude, it is nevertheless felt that the image amplification properties of a TWOM have been shown and that this property of the TWOM may be of importance in a communication system.

VI. IMAGE DEFINITION, CHANNEL CAPACITY AND NOISE

The capacity of a communication system depends upon the total number of unit phase-space cells which the system can handle. The usual communication system has a spatial width of only one cell (it is single mode), and information is conveyed only in the longitudinal direction — i.e., the frequency and time domain. At optical frequencies however, it may be convenient to use many cells in transverse space. A discussion is therefore given of the channel capacity of a multimode image-amplifying maser.

We define channel capacity as the product of the number of cells in transverse space and the bandwidth. The latter has been discussed earlier; it remains to consider the former.

Evidently if we are dealing with an infinitely long cylindrical amplifier

with perfectly reflecting walls — i.e., a multimode waveguide with gain — then the number of modes for a unidirectional, single-polarization amplifier is $\pi A/\lambda^2$, where A is the cross-sectional area and the channel capacity C is

$$C = \frac{\pi A}{\lambda^2} B$$

where the bandwidth B is given by (3) for a Gaussian line shape.

In practice, the amplifier is not infinitely long, and in fact the device described here has a length $< (A/\lambda)$. Under these conditions one is concerned with the near field region of the amplifier aperture, and image transmission is possible (i.e., some modes can be transmitted from input to output independently of the boundary conditions).

Consider an idealized, unidirectional, single-polarization, cylindrical amplifier as depicted in Fig. 14 of length l and cross sectional area A.

We consider first the image space. A transmitted image can occupy in transverse (i.e., x,y,P_x,P_y) space an area equal to $A\Omega$ where Ω is the angular aperture A/l^2 and $P = (h\nu/c)$ is the photon momentum. The aperture A and its associated diffraction solid angle $\omega = \lambda^2/A$ define the transverse dimensions of a unit cell.[11] Consequently the total number of image cells available is

$$\frac{\Omega}{\omega} B\Delta t = \frac{A^2}{l^2\lambda^2} B\Delta t \tag{12}$$

where Δt is the time over which the observation is made. Equation (12) may be interpreted to mean: (*i*) that Ω/ω identifiable image points can be amplified (this also follows from classical diffraction considerations) and (*ii*) that the image channel capacity $\Delta C = (\Omega/\omega)B$. The device whose operation has been described here has a $\Delta C \approx 3 \times 10^{15}$ cps.

One can classify cells into groups according to the behavior of their corresponding rays of geometric optics. Those used for transmitting an image consist of $A^2/l^2\lambda^2$ rays which pass directly from the input to the

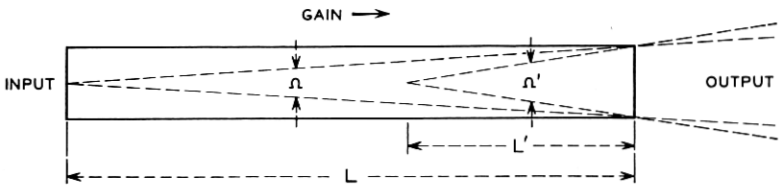

Fig. 14 — An idealized image amplifier.

output. The next group consists of $3(A/l^2\lambda^2)$ rays which undergo a single internal reflection at the wall before reaching the output and fall within the solid angle 4Ω minus the image core Ω. Successive groups undergo an increasing number of internal reflections. The reason for the A^2 dependence in (12) is now clear — the area and consequently the total number of cells which the transmission line can support is proportional to A, and out of this total number, that fraction which can pass directly from input to output is also proportional to A. If the length of the amplifier is greater than A/λ, then all rays are reflected from the walls and, in this limit, one is concerned with waveguide propagation.

In principle, and to a certain extent in practice, the "off axis" rays are available for transmitting information. The internal reflections will result in image distortion, but cylindrical symmetry is preserved and spatial coding can be used. At the present time, however, the channel capacity using only the image core is embarrassingly large and there seems little advantage in using the "off axis" rays.

The limiting noise of a maser (or for that matter any coherent amplifier) corresponds to one noise photon per unit cell of phase space, (noise number[12] $N = 1$). Optical masers can come very close to this limit and in fact the ruby amplifier described in this paper has a calculated $N \approx 2$. The number of noise photons associated with the signal is consequently $N\ \Delta C$.

In the frequency domain it is well known that there is an optimum bandwidth for a given signal and that excess bandwidth gives excess noise. Similarly in the transverse domain there is an optimum spatial bandwidth; in particular the angular aperture Ω used should not exceed that required for the necessary definition, as this would add excess noise. If the amplifier has excess angular aperture, the optics should be arranged so that the transmitted image and the following receiver occupy only the necessary solid angle.

In practice, additional noise is produced at the output, and proper precautions should be taken to eliminate this excess noise. Consider first only the noise associated with image rays. A cross section along the amplifier, shown dotted in Fig. 14, may be considered as the input of the remaining part of the amplifier with a new angular aperture $\Omega' = A^2/l'$ which is larger than Ω. We have therefore an amplifier whose bandwidth (spatial) increases (to a limit $\Omega' = 2\pi$) as we travel along the device. Excess noise will appear at the output in this larger solid angle but will of course see less gain than that in the useful angle Ω. A detector, insensitive to angle, placed at the output will see this noise, which can be severe in some designs. This excess noise, which is not intrinsic to the

signal band, can perhaps most easily be eliminated by focussing the input plane on the detector and using an aperture stop which passes only the focused image.

Even though one may not intend to use the "off axis" rays they may, unless special precautions are taken, be available at the output. Commonly used solid-state maser materials have large indices of refraction and, consequently, internal reflections may occur for large angles of incidence (for ruby the critical angle is $\approx 60°$). It is evident, therefore, that an appreciable fraction of the spontaneously emitted photons can be amplified and reach the output. These can be separated from those in the signal image core by the method mentioned above.

One should differentiate between presently available image intensifiers and maser image amplifiers. Unlike the maser, the former are not coherent amplifiers and are perhaps better described as image quantum detectors. The quantum detector preserves the intensity of the signal but not its phase (and in practice it is difficult to preserve the momentum). The maser preserves both amplitude and phase and easily preserves the frequency and direction of the signal. It is a direct consequence of uncertainty that a coherent amplifier has a noise number $N \geqq 1$. The detector which preserves only one variable can in principle be noise free, although this does not mean that it is more "sensitive" than a maser in some systems applications.[13]

At wavelengths of $< 1\mu$ the black body temperature of an object must be $> 10^4$°K before the phase-space density can exceed unity. As a consequence, the phase of the radiation is indeterminate for objects illuminated by usual incoherent light sources. There appears little object in using a coherent amplifier with such an image, and in fact its noise can be a serious disadvantage.

If an object is illuminated by a maser oscillator, however, then densities $\gg 1$ can be obtained, and in fact densities > 1 are necessary in a communication system in order to make full use of channel capacity. In such systems a coherent image amplifier which can also easily preserve the frequency, phase and direction of a signal may be of value.

VII. PUMP POWER REQUIREMENTS

One of the principal practical difficulties associated with optical masers is that of providing the pump. Minimum pump power and minimum pump color temperature are mutually exclusive, and in practice a compromise must be reached. In this section we are concerned with the effects of signal circuit design on the pump requirement of a CW

amplifier. It is clear that with the use of materials whose quantum efficiency is near unity (ruby has a Q.E. ≈ 0.9) pump photons are required only to replace those photons dissipated at the signal transition. In practice, signal circuit design can affect the pump requirements by several orders of magnitude.

The total number of photons emitted at the signal transition from an uncertainty-limited ($N = 1$) maser amplifier is

$$N_T = \sum \left(\frac{c^3}{8\pi\nu^2} \frac{G_0 - 1}{\ln G_0} \frac{n}{\tau} + G_0 D \right). \tag{13}$$

Here G_0 is the numerical gain for a given cell and D the dynamic range (equal to the maximum number of photons per cell in the input signal). n is the density of particles per unit volume per spectral interval, and from the previous equations n/τ is related to G_0. The first term is due to spontaneous emission and amplified spontaneous emission, and the second is due to the amplified signal. Equation (13) may conveniently be regrouped as

$$N_T = \sum_{\substack{\text{All Signal} \\ \text{Cells } \Delta C}} \left(\frac{c^3}{8\pi\nu^2} \frac{G_0 - 1}{\ln G_0} \frac{n}{\tau} + G_0 D \right) + \sum_{\text{The Remainder}} \frac{c^3}{8\pi\nu^2} \frac{G_0 - 1}{\ln G_0} \frac{n}{\tau}. \tag{14}$$

The first term is determined entirely by the specifications placed on the amplifier; i.e., it has a channel capacity ΔC, a gain G_0, and a dynamic range D over this band. The first part accounts for the noise from an uncertainty-limited amplifier. The second part is due to the signal. When $G_0 \& D \gg 1$, the first term becomes $G_0 \Delta C D$. The second term is the sum, over all other cells into which the particles can radiate, of the spontaneously emitted and amplified spontaneously emitted photons. This term, which is concerned with cells outside the signal band, represents wasted energy. If ΔC contains only a small fraction of the total number of cells, this term may be approximated as $K(N/\tau)$ where N is the total number of particles at the signal transition and K is the average of $(G_0 - 1)/(\ln G_0)$. Evidently if the gain for these excess cells is unity, then the second term is just N/τ, the total spontaneous emission.

In a practical amplifier it seems likely that the specifications and the design will be such that (14) will be represented to a good approximation by

$$N_T = G_0 \Delta C D + K N/\tau. \tag{15}$$

Certainly it is likely that a $G_0 \& D \gg 1$ will be required and hence the

first part is a good approximation. If $G_0 \& D \gg 1$, then an insignificant amount of pump power will be saved by designing so that ΔC occupies an appreciable fraction of the total phase space and further, since such a design would appreciably increase the pump color temperature requirements, it seems likely that the fraction will be kept small. Under these circumstances, the second part is also a good approximation. A signal circuit efficiency η_s may then be defined as

$$\eta_s = G_0 \Delta C D / (G_0 \Delta C D + K N/\tau). \tag{16}$$

The preceding discussion is now applied to a single-mode transmission system — i.e., one where the information is to be sent only in the longitudinal domain. An obvious design for an amplifier in this application might be a single-mode, single-polarization waveguide TWM using fibre optics. A material with a quantum efficiency near unity, an inversion near 100 per cent, and a signal linewidth just sufficient to give the required bandwidth might be used. As far as the material and signal structure is concerned, such a design has 100 per cent photon efficiency; i.e., every photon absorbed from the pump is available for amplification at the signal frequency and in the signal mode. (To be strictly correct, the efficiency is 25 per cent if it is a single-polarization, unidirectional amplifier.) The ratio of stimulated to spontaneous emission is $\approx [(G_0 - 1)/\ln G_0]$ for high gain in the absence of a signal. If the requirement was for a gain of 30 db then this ratio is $\approx$20 db. Further since one-half of the stimulated emission photons will be produced in the last 3 db (10 per cent of the length) of the amplifier, the rate at which photons are produced at the output section is $\approx 10^3$ times that from spontaneous emission alone. This means that the idler relaxation time must be $< 10^{-3}$ of the spontaneous emission lifetime and that the pump density must be 10^3 greater than that required to produce the same inversion in the absence of gain. So far we have considered only the contribution from amplified noise. If in addition we require that the device be able to amplify a signal $D \times$ noise, the above figures of 10^{-3} and 10^3 become 10^{-5} and 10^5, respectively, for $D = 20$ db. These perhaps impossible requirements on the idler relaxation time and pump color temperature have arisen because the device is too efficient.

A less efficient alternative design is now considered for the above application. Consider an image amplifier of the type depicted in Fig. 14. Since we are concerned with only one transverse mode, we need the definition for only one image point — i.e., $l \approx A/\lambda$.

Equation (15) is a good approximation in this case. The first term, which represents essential energy, is

$$G_0 \Delta CD = G_0 D \Delta \nu \sqrt{\frac{\log \dfrac{G_{\text{db max}}}{G_{\text{db max}} - 3}}{\log 2}}.$$

The second term, which represents wasted energy, is given by

$$K \frac{N}{\tau} = K \frac{n}{\tau} \times \text{volume} = K l^2 \lambda \frac{n}{\tau}.$$

Also, if W is isotropic and we have complete inversion, (2) gives

$$l = \frac{G_{\text{db}} \epsilon \Delta \nu}{0.16 \lambda^2} \frac{g_2}{g_1} \frac{\tau}{n}$$

and hence

$$K \frac{N}{\tau} = K \times \frac{G_{\text{db}}^2 \epsilon^2 \Delta \nu^2}{0.0256 \lambda^3} \left(\frac{g_2}{g_1}\right)^2 \frac{\tau}{n}.$$

As in the last example we assume the amplifier is required to have a gain of 30 db and a dynamic range of 20 db. If 0.05 per cent ruby is used at room temperature, if complete inversion is obtained and if further we assume that, contrary to the device described in this paper, the isolators use a negligible fraction of the total length, then

$$\Delta C \approx 10^{11} \text{ cps}$$

giving

$$G_0 \Delta CD \approx 10^{16} \text{ photons per sec}$$

also

$$l \approx 16 \text{ cm}$$

giving

$$K \frac{N}{\tau} \approx 0.85 \times 10^{20} K \text{ photons per sec.}$$

From (16) the structure efficiency is

$$\eta_s \approx \frac{1}{K} 1.2 \times 10^{-4}.$$

Since the signal is capable of interacting with almost all of the spins, the signal photon density has negligible effect upon the required pump color temperature with this value for η_s. It is essential to keep K small since it has a direct effect on the required color temperature as well as

on the required pump power. The index of refraction of most solid-state maser materials is so large that unless special precautions are taken to prevent internal reflections, a large fraction of the off-axis rays will see the full amplifier gain. This could easily lead to a value for $K \approx 100$ for a 30-db amplifier with a corresponding two order-of-magnitude increase in the required pump power and energy density. An estimate indicates that it should be possible to keep $K < 2$ with correspondingly little effect on the power and density of the pump.

The two amplifiers just described represent design extremes. The single-mode waveguide amplifier has a minimum pump power but an excessively high pump density requirement (in this example 5 orders of magnitude above that for spontaneous emission alone). Conversely the single-cell image amplifier has a minimum pump density but an excessive pump power requirement (in this example 4 orders of magnitude above that intrinsic to the specifications). A reasonable compromise objective might be for $\eta_s \approx 50$ per cent, in which case both the power and density requirements would both be increased only by a factor of 2 from the minimum.

The single-cell image amplifier just described is very inefficient because only a small fraction of the total phase space is available to the useful image core. A somewhat different geometry can improve this. As an example, one could break up the amplifier into say 10 sections, each with a gain of 3 db. Each section is now capable of amplifying one image point if $l/10 \approx A/\lambda$; i.e., A and hence $K(N/\tau)$ can be reduced a factor of 10 with a corresponding increase in η_s. Of course with this decrease in A, the diffraction angle is larger and unity magnification lenses must be placed between sections to reform the image at the input plane of the next section. The extent to which this subdivision can be continued is in practice limited by the fact that electronic gain per section decreases with the number of sections while the circuit loss per section will be substantially constant, leading to an eventual decrease in the net gain of the entire device.

This section has been concerned primarily with amplifiers for use in a single-mode transmission system, and the information has been conveyed in the longitudinal domain. It has been shown that pump density and power can vary over wide ranges by signal circuit design. In principle, analogous arguments apply to an image amplifier where information is to be conveyed primarily in the transverse domain: in practice, the problem is primarily one of increasing the efficiency and would appear to depend largely on obtaining narrow linewidth materials. Narrow-frequency band filters are probably also necessary to obtain high effi-

ciency. It is perhaps worthwhile noting that filters of the Fabry-Perot type are narrow in entire momentum space and as such inhibit image transmission.

VIII. RECIRCULATION

Since the amplifiers described here are traveling-wave devices, they may be folded to achieve a more desirable geometry. An extreme case of folding is to send successive signal passes through what is otherwise a single section; i.e., an amplifier is designed so that its transverse capacity exceeds that required for the signal, which may then be recirculated in this otherwise excess image space.

If, for example, one is concerned, as in the last section, with an amplifier for a single-mode transmission system, then each pass must occupy a region $\Delta x\ \Delta y\ \Delta P_x\ \Delta P_y \approx h^2$. Further it is essential to make efficient use of this transverse space if η_s is not to deteriorate. It may be necessary to provide image guard bands to inhibit feedback: the resulting decrease in η_s may in practice be more than compensated by an increase in the pump circuit efficiency with this geometry.

The recirculating optics can take many forms. Rectilinear reflections can produce the simple single-cell image amplifier described in the last section in compact form. The addition of lenses can produce the folded equivalent of the third type of amplifier described in the last section. If a Faraday rotation isolator is used, an optically active material such as quartz in the recirculating path can restore the polarization. The number of passes is limited by the losses in the optics and by the amount of feedback which can be tolerated.

IX. TRANSIENT BEHAVIOR

The fact that a TWM can store energy and release it on demand is well known. This property has been of only academic interest at microwave frequencies but may be one of the most important characteristics of an optical device. The transient behavior of a TWM has been investigated by Schulz-DuBois[6] and may be summarized as follows. If a strong signal in the form of a step function is applied, then the leading edge will see the full amplifier gain and, in the process, will drain off active particles so that successive portions of the signal experience less gain. As the signal travels along the amplifier, it assumes somewhat the shape of a shock wave where the sharp leading edge sees the full gain, and the integrated energy in the pulse is essentially equal to the original stored energy in the preceding portion of the amplifier. The output pulse

width is limited by the rise time of the amplifier. This theory is valid as long as the material characteristics at the signal frequency can be described in terms of the rate equations.

The rise time of a ruby TWOM at room temperature is $\approx 2 \times 10^{-12}$ sec. By using the pulse-sharpening property of the device, it may be possible to produce light pulses shorter than any available by conventional electronics.

It is easy to design a TWOM of cross section less than 1 cm^2 whose stored energy is greater than one joule. With such a device, rise time is unlikely to limit the peak power; instead, the limitation will probably be material breakdown. In the present design the Polaroid is believed to be the most susceptible component but could be replaced by, say, Glan-Thomson or Brewster angle polarizers. We expect that peak powers of 10^7 watts/cm^2 can be achieved quite easily without focusing and that considerably higher power densities are realizable.

Once the limiting power density and cross-sectional area are reached, the beam can be divided into parallel channels forming a phased array. If phase stabilities approaching that of the microwave TWM can be achieved, several divisions will be possible.

X. CONCLUSION

The feasibility of an image-amplifying optical traveling wave maser has been demonstrated. Since each section is short circuit stable, they may be cascaded to produce any desired gain.

The experimental data on the gain as a function of pump power are in good agreement with theory.

The loss and Verdet constant of high density PbO glass has been measured and is such that in combination with dichroic polarizers it leads to a satisfactory isolator. Materials with higher Verdet constants would be preferable.

The theory shows that, in order to build an amplifier which is low noise and which has a minimum pump requirement, one must use high quality optics which are diffraction limited.

It is believed that very high peak powers and very short pulses can be produced with the device.

An effective channel capacity $\approx 10^{15}$ cps has been obtained and one is faced with the rather unusual problem of reducing the bandwidth of an amplifier.

XI. ACKNOWLEDGMENTS

The authors wish to acknowledge the assistance of Mr. H. Marcos in making the measurements on the optical isolator. We also are in-

debted to our colleagues Dr. E. O. Schulz-DuBois and Dr. J. G. Skinner for critically reading the manuscript and making valuable suggestions.

REFERENCES

1. Maiman, T. H., Nature, **187,** 1960, p. 493.
2. Javan, A., Bennett, W. R., Jr., and Herriott, D. R., Phys. Rev. Letters, **6,** 1961, p. 106.
3. Javan, A., Bennett, W. R., Jr., and Ballik, E. A., private communication.
4. Kisliuk, P. P., and Boyle, W. S., Proc. I.R.E., **49,** 1961, pp. 1635–1639.
5. DeGrasse, R. W., Schulz-DuBois, E. O., and Scovil, H. E. D., B.S.T.J., **38,** 1959, pp. 305–334.
6. Schulz-DuBois, E. O., Microwave Solid-State Devices, *11th Interim Report*, Army Signal Corps Contract DA-36-039-sc-73224.
7. Condon, E. U., and Shortley, G. H., *The Theory of Atomic Spectra*, Cambridge University Press, London and New York, 1951.
8. Wieder, I., and Sarles, L., *Advances in Quantum Electronics*, edited by J. R. Singer, Columbia University Press, New York, 1961.
9. Schawlow, A. L., *Advances in Quantum Electronics*, edited by J. R. Singer, Columbia University Press, New York, 1961.
10. McClure, D. S., *Advances in Solid State Physics*, **9,** edited by F. Seitz and D. Turnbull, Academic Press, Inc., New York, 1959.
11. Dirac, P. A. M., *Quantum Mechanics*, 3rd edition, Oxford University Press, 1947, p. 238.
12. Weber, J., Masers, Rev. Mod. Phys., **31,** 1959, p. 681.
13. Gordon, J. P., to be published in Proc. I.R.E.